



Highest recorded electrical conductivity and microstructure in polypropylene–carbon nanotubes composites and the effect of carbon nanofibers addition

C. A. Ramírez-Herrera¹ · J. Pérez-González² · O. Solorza-Feria³ · N. Romero-Partida⁴ · A. Flores-Vela⁵ · J. G. Cabañas-Moreno¹

Received: 14 March 2018 / Accepted: 26 March 2018 / Published online: 6 April 2018
© Springer-Verlag GmbH Germany, part of Springer Nature 2018

Abstract

In the last decade, numerous investigations have been devoted to the preparation of polypropylene–multiwalled carbon nanotubes (PP/MWCNT) nanocomposites having enhanced properties, and in particular, high electrical conductivities ($> 1 \text{ S cm}^{-1}$). The present work establishes that the highest electrical conductivity in PP/MWCNT nanocomposites is limited by the amount of nanofiller content which can be incorporated in the polymer matrix, namely, about 20 wt%. This concentration of MWCNT in PP leads to a maximum electrical conductivity slightly lower than 8 S cm^{-1} , but only by assuring an adequate combination of dispersion and spatial distribution of the carbon nanotubes. The realization of such an optimal microstructure depends on the characteristics of the production process of the PP/MWCNT nanocomposites; in our experiments, involving composite fabrication by melt mixing and hot pressing, a second re-processing cycle is shown to increase the electrical conductivity values by up to two orders of magnitude, depending on the MWCNT content of the nanocomposite. A modest increase of the highest electrical conductivity obtained in nanocomposites with 21.5 wt% MWCNT content has been produced by the combined use of carbon nanofibers (CNF) and MWCNT, so that the total nanofiller content was increased to 30 wt% in the nanocomposite with PP—15 wt% MWCNT—15 wt%CNF.

Keywords Polymer nanocomposites · Carbon nanotubes · Carbon nanofibers · Polypropylene nanocomposites · Electrical properties

Introduction

In the past few decades, there has been a great expansion in research related to polymer nanocomposites for potential applications in different fields such as electronic devices, energy storage, sensors, electrostatic discharge and electromagnetic interference shielding, and biomedical applications (Kurahatti et al. 2010; Njuguna et al. 2012; Das and Prusty 2013; Müller et al. 2017). A large part of this interest has been focused on polymers with improved electrical, mechanical and thermal properties, as a result of the combination with carbon-based nanomaterials including single- and multi-wall (MWCNT), carbon nanofibers (CNF), graphene, and graphite nanoplatelets, among others (Kurahatti et al. 2010; Spitalsky et al. 2010; Njuguna et al. 2012; Müller et al. 2017; Al-Saleh and Sundararaj 2009; Tibbetts et al. 2007; Kim et al. 2010; Das and Prusty 2013). These additions lead in most cases to significant improvements in the mechanical and physical properties of the polymer

✉ C. A. Ramírez-Herrera
caramirez@cinvestav.mx

¹ Programa de Doctorado en Nanociencias y Nanotecnología, CINVESTAV, Av. Instituto Politécnico Nacional 2508, C.P. 07360 Ciudad de México, Mexico

² Departamento de Física, Escuela Superior de Física y Matemáticas, Instituto Politécnico Nacional, Av. Instituto Politécnico Nacional s/n, C.P. 07738 Ciudad de México, Mexico

³ Departamento de Química, CINVESTAV, Av. Instituto Politécnico Nacional 2508, C.P. 07360 Ciudad de México, Mexico

⁴ Industrias Romfer S.A. de C.V., Sierravista 298, C.P. 07300 Ciudad de México, Mexico

⁵ Centro Mexicano para la Producción más Limpia, Instituto Politécnico Nacional, Av. Acueducto s/n, C.P. 07340 Ciudad de México, Mexico

composites at lower filler contents compared to other, more commonly used carbonaceous fillers (Zhou et al. 2006; Deng et al. 2009; Li et al. 2011; Njuguna et al. 2012; Garzón and Palza 2014), like graphite (G) and carbon black (CB). Also, from a practical point of view, smaller filler loads also facilitate the processing of the composite material.

A wide range of thermoplastics, including polypropylene (PP), poly(methyl methacrylate), polyethylene, polystyrene and polycarbonate have been combined with carbonaceous nanofillers. In particular, PP, a nonpolar semi-crystalline polymer, is one of the most used thermoplastics in composite fabrication because of its high corrosion and heat resistance, low density, excellent formability and processability, and low cost (Kissel et al. 2003). There exist a large number of publications dealing with the processing, properties and modeling of PP/MWCNT nanocomposites (Zhou et al. 2006; Tjong et al. 2007; Mičušík et al. 2009; Bauhofer and Kovacs 2009; Logakis et al. 2010; Pan et al. 2010; Xin and Li 2012; Pan and Li 2013; Shehzad et al. 2013; Garzón and Palza 2014; Park et al. 2014; Verma et al. 2015; Al-Saleh 2015, 2016; Cesano et al. 2016), not to mention nanocomposites of PP/CB, PP/G and PP/CNF (Chodák et al. 2001; Zhou et al. 2006; Deng et al. 2009; Merzouki and Haddaoui 2012; Bao et al. 2013; Tchmutin et al. 2003; Al-Saleh and Sundararaj 2009; Tibbetts et al. 2007; Li et al. 2011). In many cases, remarkable mechanical, physical and chemical properties have been reported with the addition of relatively low amounts of MWCNT; however, it is clear that most properties are heavily dependent on the microstructure of the nanocomposites, from the mesoscopic to the nanoscopic scale, which is of course controlled by the processes employed in nanocomposite production.

In the present work, our interest especially resides on the maximum electrical conductivity attainable in PP/MWCNT nanocomposites. In this case, it turns out that the limitations are ultimately imposed by the maximum amount of nanofiller content which can be incorporated in the PP matrix. It is not coincidental that the highest MWCNT loads reported in different publications on PP/MWCNT nanocomposites are ~20% in weight (Zhou et al. 2006; Mičušík et al. 2009; Pan et al. 2010; Pan and Li 2013; Shehzad et al. 2013; Park et al. 2014; Verma et al. 2015; Al-Saleh 2015, 2016); in practice, it is extremely difficult to add a higher amount of MWCNT to a given mass of PP, because the effective MWCNT volume becomes larger than the corresponding volume of the polymer.

An alternative way to increase the electrical conductivity of PP/MWCNT is to use two or more different nanofillers, i.e., by producing hybrid nanocomposites. There are numerous indications that a synergistic effect may be found in such cases (Li et al. 2008; Sun et al. 2009; Garzón and Palza 2014; Liu et al. 2014; Sharma et al. 2016; Lin et al. 2016); but, again, there is a wide variation in

the reported results concerning the properties found in hybrid nanocomposites in which MWCNT is one of the nanofillers in use. Evidently, considering all the possible carbon-based nanofillers and their varying proportions in the nanocomposite, as well as the different processing methods available, there remains much to be explored in terms of composition-processing-microstructure and properties in hybrid nanocarbon-filled polymer composites.

Whether single or multiple nanofillers are used, the microstructural effect on the electrical properties of the nanocomposites is of paramount importance (Al-Saleh and Sundararaj 2009; Bauhofer and Kovacs 2009; Mičušík et al. 2009; Sun et al. 2009; Bikiaris 2010; Pan et al. 2010; Merzouki and Haddaoui 2012; Xin and Li 2012; Pan and Li 2013; Cesano et al. 2016). This effect has been clearly demonstrated a number of times in studies of the percolation threshold of PP/MWCNT and other types of nanocomposites (Tjong et al. 2007; Bauhofer and Kovacs 2009; Pan and Li 2013; Park et al. 2014; Cesano et al. 2016; Bao et al. 2013). However, the nanofiller content to reach electrical percolation is usually of a few weight percent and the electrical conductivity values in PP/MWCNT nanocomposites with such reduced amounts of nanofiller is usually under 10^{-2} to 10^{-3} S cm⁻¹ (Spitalsky et al. 2010; Bauhofer and Kovacs 2009). In the case of the onset of percolation phenomena, it is generally considered that MWCNT are most effective when they are disentangled and homogeneously dispersed over the whole volume of the polymer matrix. As will be shown, the electrical conductivity in PP/MWCNT nanocomposites can be augmented to about 10 S cm⁻¹ with increasing nanofiller loads, but in this case the higher conductivities require a microstructure in which MWCNT aggregates form a continuous network within the matrix; in other words, electrical conductivity of the order of 1–10 S cm⁻¹ requires not only that an electrical pathway is established throughout the volume, but, most importantly, that a large fraction of the MWCNT is performing as conductors at an given time.

In the present work, PP/MWCNT and PP/MWCNT/CNF nanocomposites have been prepared using different loadings of MWCNT and CNF. The emphasis is on PP/MWCNT composites and the attainment of a high electrical conductivity (> 1.0 S cm⁻¹). It will be shown that maximum in-plane electrical conductivity is about 7 S cm⁻¹ with a MWCNT content of about 20 wt%, but it is only about 0.2 S cm⁻¹ for through-plane electrical conductivity. Some preliminary experiments indicate that, with MWCNT content restricted to a maximum of 20 wt%, higher conductivities may be obtained by recurring to hybrid PP/MWCNT/CNF nanocomposites in which the maximum total nanofiller content can be increased to about 30 wt%.

Experimental

Materials

Commercial grade polypropylene, PP 4280 W Impact copolymer (supplied by Total Petrochemicals), with melt flow index = $1.3 \text{ g (10 min)}^{-1}$, was used as the polymer matrix. As electrically conductive fillers, the materials used were (i) MWCNT (cat. number 773840 from Sigma-Aldrich) with a purity $\geq 98\%$, average outside diameter of 10 nm, length of 3–6 μm , and (ii) Pyrograf[®]-III CNF (cat. number 719781 from Sigma-Aldrich) with outside diameters and lengths ranging from 125 to 150 nm and 20 to 200 μm , respectively.

Preparation of hybrid polymer nanocomposites

PP pellets were ground in a laboratory mill and a 2-mm sieve was used to separate fine PP particles. The sieved powders were pre-mixed with different amounts of MWCNT and CNF in an 8000 M Mixer/Mill[®] High-Energy Ball Mill (SPEX[®] SamplePrep, USA). Table 1 shows the formulations of the PP/MWCNT and PP/MWCNT/CNF blends that were prepared. After the pre-mixing process, the corresponding nanocomposites were produced by melt mixing in a Brabender mixer equipped with a pair of high-shear roller-type rotors and coupled to a Brabender Plasti-Corder[®] PL-2100 Torque Rheometer System (C.W. Brabender Instruments, Inc., USA), using a rotation speed of 90 rpm at 230 °C for 30 min. The maximum total loading of nanofillers used was 30 wt%. The resulting composites were molded by compression into plates of approximately 1.5 mm thickness for subsequent characterization. Additionally, the most conductive samples were later subjected to a reprocessing stage which consisted of re-melting at 200 °C followed by compression

Table 1 Formulations (weight %) of PP/MWCNT and PP/MWCNT/CNF nanocomposites

Material ID*	PP	MWCNT	CNF
PP/5MWCNT	95	5	0
PP/10MWCNT(– R)	90	10	0
PP/15MWCNT(– R)	85	15	0
PP/20MWCNT(– R)	80	20	0
PP/21.5MWCNT(– R)	78.5	21.5	0
PP/20CNF(– R)	80	0	20
PP/10MWCNT/10CNF(– R)	80	10	10
PP/15MWCNT/15CNF(– R)	70	15	15

*(- R) indicates samples that were additionally subjected to reprocessing

into plates of thicknesses between 0.1 and 0.2 mm. The reprocessed samples are identified by adding (– R) at the end of the identification term (e.g., PP/20MWCNT-R).

Characterization

The cryo-fractured surfaces of all the specimens were observed using field-emission scanning electron microscopy (SEM) under acceleration voltages of 1.0–1.5 kV (Auriga 3916, Carl Zeiss, Germany and JSM 7800F, JEOL, USA). Large area (about $220 \times 220 \mu\text{m}^2$) observations of the microstructure of the nanocomposites were realized by confocal laser scanning microscopy (CLSM), using a multiphoton confocal microscope (LSM710-NLO, Carl Zeiss, Germany). Previous studies have used CLSM to assess the volumetric dispersion and distribution of nanofillers in polymer matrices by looking at the direct laser reflection from aggregates of nanofillers (Yazdani et al. 2014; Smith et al. 2015; Reyes-Acosta et al. 2015; Ilčíková et al. 2016).

The in-plane electrical conductivity of the nanocomposites was measured by the four-point probe (FPP) method at room temperature. In this technique, four equally spaced probes in a linear arrangement are gently placed in contact with the surface material, as shown schematically in Fig. 1a. The two outer probes are used to conduct a current from the source, while the two inner probes measure the resulting voltage drop across the surface of the sample. The relationship of the current and voltage values obtained depends on the resistivity of the material under test and the geometrical characteristics of the probes. For nanocomposites with electrical resistance higher than $10^3 \Omega$, a Lucas Labs Pro-4 Resistivity System (Lucas Signatone Corp., USA), equipped with a Keithley Model 2400-C SourceMeter[®], was used. Nanocomposites with resistance values below $10^3 \Omega$ were tested in a Four Probe Set-up DFP-02 (SES Instruments Pvt. Ltd., India), equipped with a multirange digital voltmeter (0–200 mV) and a constant current generator (0–20 mA). Unless otherwise indicated, measurements were done on specimens having dimensions of $10 \times 10 \times 1.5 \text{ mm}^3$. The average value of five readings at different locations for each sample was taken as the resistance (R , in Ω) of the nanocomposite. According to the FPP method (Schroder 2006), for a rectangular specimen of finite thickness w (in cm), the resistivity (ρ , in $\Omega \text{ cm}$) is calculated as:

$$\rho = \frac{\pi}{\ln 2} \cdot w \cdot R \cdot F_1 \cdot F_2, \quad (1)$$

where F_1 and F_2 are geometric correction factors (Schroder 2006). Values of the electrical conductivity (σ , in S cm^{-1}) were obtained by inverting the corresponding values of ρ :

$$\sigma = \frac{1}{\rho}. \quad (2)$$

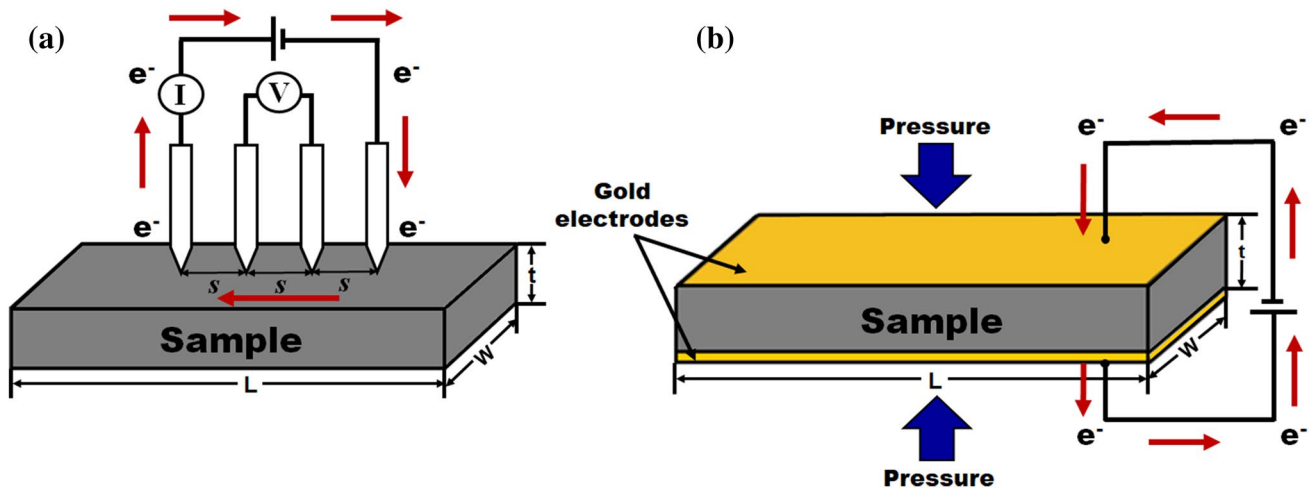


Fig. 1 a Schematic representation of measurements of in-plane and b through-plane electrical conductivity on the nanocomposite samples

The through-plane electrical conductivity provides information of the electrical characteristics at locations deeper inside the material. The measurements of through-plane electrical properties of the nanocomposites were determined by electrochemical impedance spectroscopy (EIS) using an Autolab PGSTAT302N potentiostat/galvanostat (Metrohm Autolab B. V., Netherlands). In this method, samples with dimensions of $10 \times 10 \times 1.5 \text{ mm}^3$ were pressed between two gold electrodes as shown in Fig. 1b. A sinusoidal perturbation electric potential, E , of variable frequency, ω , was applied to the system, and a current signal, i , was recorded. From this, the impedance of the system $Z(\omega)$ can be calculated using Ohm's law as:

$$Z(\omega) = \frac{E(\omega)}{i(\omega)}. \quad (3)$$

EIS measurements were carried out over the wide frequency range of 10^{-2} to 10^6 Hz. By means of the NOVA 2.1 software (NOVA 2.1 2016, Metrohm Autolab B.V.), plots of frequency vs. impedance/AC resistance, Z , were obtained. The through-plane electrical conductivity (σ , S cm^{-1}) was calculated from the AC resistance values (R , in Ω) as:

$$\sigma = \frac{w}{R \cdot A}, \quad (4)$$

where w and A are, respectively, the thickness (in cm) and the area (width \times length, in cm^2) of the sample, and R is taken as the value of Z when it becomes independent of frequency. It was found that the calculated conductivity values for reprocessed samples varied considerably with sample thickness; therefore, the results of such measurements are not reported in the present work.

Results and discussion

PP/MWCNT nanocomposites

Figure 2a shows the in-plane electrical conductivity of the PP/MWCNT nanocomposites as a function of nanofiller content. According to the supplier, the electrical conductivity of the PP used in this study is about $1 \times 10^{-16} \text{ S cm}^{-1}$. As shown in this figure, PP/MWCNT nanocomposites exhibit the expected trend of increasing electrical conductivity with MWCNT content. In the initially processed materials, the conductivity is raised by more than 11 orders of magnitude, to $5.6 \times 10^{-5} \text{ S cm}^{-1}$, with the addition of 5 wt% MWCNT (see Table 2). Increasing the amount of MWCNT from 5 to 21.5 wt%, increases the electrical conductivity of these nanocomposites by an additional 5 orders of magnitude, reaching a maximum value of 1.9 S cm^{-1} . In turn, as shown in Fig. 2a, the electrical conductivity of the reprocessed nanocomposites increased by an additional one to two orders of magnitude. The highest in-plane electrical conductivity recorded for PP/MWCNT nanocomposites was 6.7 S cm^{-1} (Table 2), corresponding to the PP/21.5MWCNT-R nanocomposite; this value is a factor of three higher than the value recorded for the original PP/21.5MWCNT nanocomposite.

Values of in-plane electrical conductivity previously reported in the literature for PP/MWCNT nanocomposites are shown in Fig. 2b. There are relatively few studies including MWCNT contents equal or larger than 10 wt% (Zhou et al. 2006; Mičušík et al. 2009; Pan et al. 2010; Pan and Li 2013; Park et al. 2014; Verma et al. 2015; Al-Saleh 2015, 2016). For clarity, the results of the present work on similar materials are again included in Fig. 2b. Notice that there are differences of 3–4 orders of magnitude between the highest and lowest conductivity values reported for PP/MWCNT nanocomposites with filler contents of 10 and

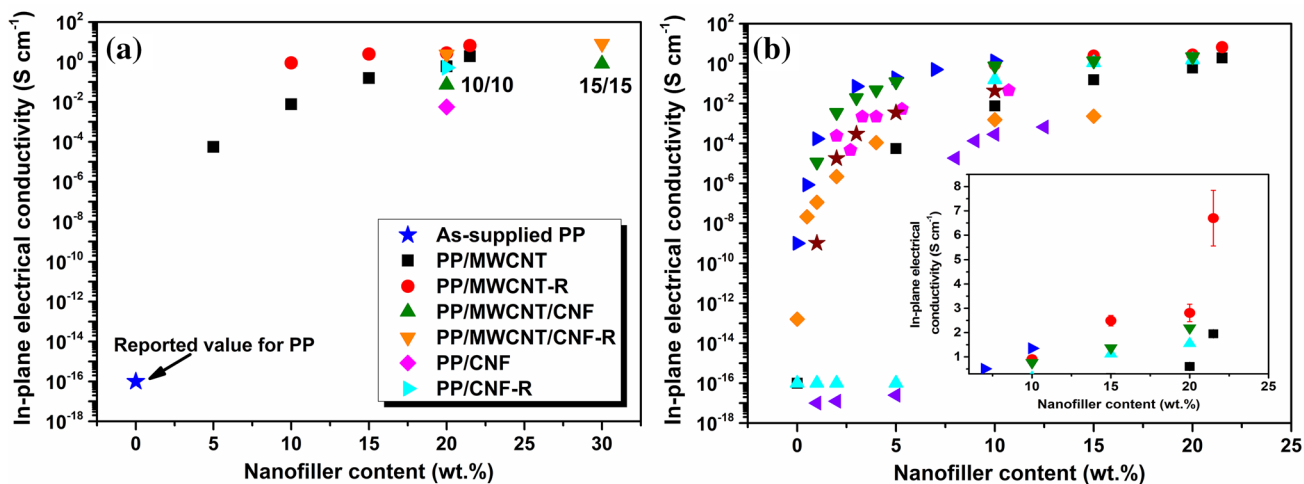


Fig. 2 **a** Measured in-plane electrical conductivity of PP/MWCNT and PP/MWCNT/CNF nanocomposites (present work). **b** Comparison with previous reports by (◀) Zhou et al. (2006), (◆) Mičušík et al. (2009), (★) Pan et al. (2010), (▶) Pan and Li (2013), (▲) Park

et al. (2014), (◇) Verma et al. (2015) and (▼) Al-Saleh (2015). The inset shows a zooming view in a linear scale of the electrical conductivity for values > 10⁻¹ S cm⁻¹

Table 2 Average values of in-plane and through-plane electrical conductivity of PP/MWCNT and PP/MWCNT/CNF nanocomposites

Material	Electrical conductivity, σ (S cm ⁻¹)		
	In-plane	In-plane (reprocessed)	Through-plane
PP/5MWCNT	5.6×10^{-5}	Not measured	1.5×10^{-5}
PP/10MWCNT	7.6×10^{-3}	9.0×10^{-1}	2.9×10^{-3}
PP/15MWCNT	1.6×10^{-1}	2.5×10^0	1.7×10^{-2}
PP/20MWCNT	6.1×10^{-1}	2.8×10^0	5.1×10^{-2}
PP/21.5MWCNT	1.9×10^0	6.7×10^0	2.4×10^{-1}
PP/20CNF	5.6×10^{-3}	5.2×10^{-1}	1.1×10^{-3}
PP/10MWCNT/10CNF	7.2×10^{-2}	2.4×10^0	6.0×10^{-3}
PP/15MWCNT/15CNF	8.1×10^{-1}	8.2×10^0	7.0×10^{-2}

15 wt%; values for a nanocomposite with 20 wt% MWCNT have only been previously presented by Park et al. (2014) and Al-Saleh (2015, 2016).

Figure 3 shows the frequency dependence of the impedance module, Z (which in AC measurements is equivalent to the resistance), of the PP/MWCNT and PP/MWCNT/CNF nanocomposites. As can be seen, the sample with lowest MWCNT content exhibits impedance values, Z , independent of frequency up to a value of about 100 kHz and then decreases with increasing frequency. Samples with higher MWCNT contents display a constant value of Z over the whole frequency range used in our measurements, a feature which is characteristic of conductive materials. It is also observed in Fig. 3 that the impedance decreases as the MWCNT content in the nanocomposite increases. This behavior has been previously reported by Logakis et al. (2010) for PP/MWCNT nanocomposites, although of considerable lower nanofiller content. From the values of Z independent of frequency in Fig. 3, through-plane electrical

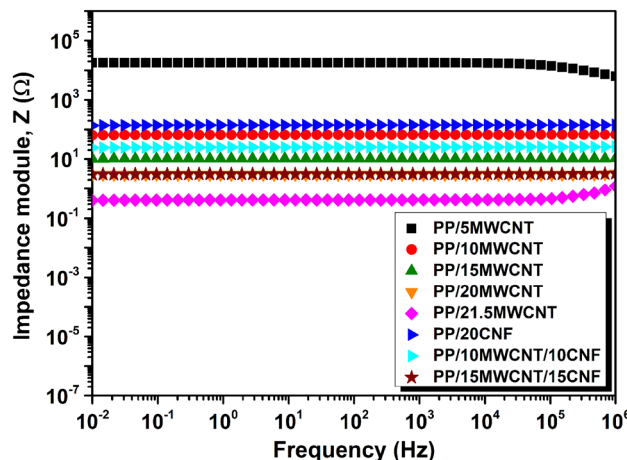


Fig. 3 Impedance module of PP/MWCNT and PP/MWCNT/CNF nanocomposites. The curves of PP/20MWCNT and PP/15MWCNT/15CNF are overlapped

conductivities were calculated for each nanocomposite and are shown in Fig. 4 and Table 2. In the latter figure, we also include values of conductivity reported by other authors (Tjong et al. 2007; Logakis et al. 2010; Shehzad et al. 2013).

From the through-plane electrical conductivity data of PP/MWCNT samples (Fig. 4), the first observation is that the AC conductivity also increases with increasing MWCNT content. In addition, the calculated through-plane electrical conductivities (Table 2) are always smaller than the corresponding in-plane values, usually by at least one order of magnitude. This last observation has also been documented in a few previous works (Tjong et al. 2007; Logakis et al. 2010; Shehzad et al. 2013); however, the comparison with results of other investigators is rather limited because of the scarcity of through-plane electrical conductivity data for MWCNT contents higher than 10 wt%.

The analysis of the electrical conductivity data for PP/MWCNT nanocomposites in Figs. 2 and 4 leads to the following conclusions: (i) large differences in conductivity in materials with nominally identical compositions should arise mainly from microstructural differences (dispersion and distribution of MWCNT); (ii) the maximum in-plane electrical conductivity attainable in PP/MWCNT nanocomposites is probably slightly below 10 S cm^{-1} and is limited by the maximum amount of MWCNT that can be added to the polymer matrix during processing ($\sim 20 \text{ wt}\%$).

Microstructural observations of the PP/MWCNT nanocomposites are illustrated in Figs. 5 and 6. First, the secondary electron images of cryo-fractured surfaces are shown in Fig. 5. Figure 5a corresponds to a reference PP specimen without any addition which displays a relatively smooth fracture surface with only a few folds due to the plasticity of PP. The images of PP/MWCNT nanocomposites (Fig. 5b–f)

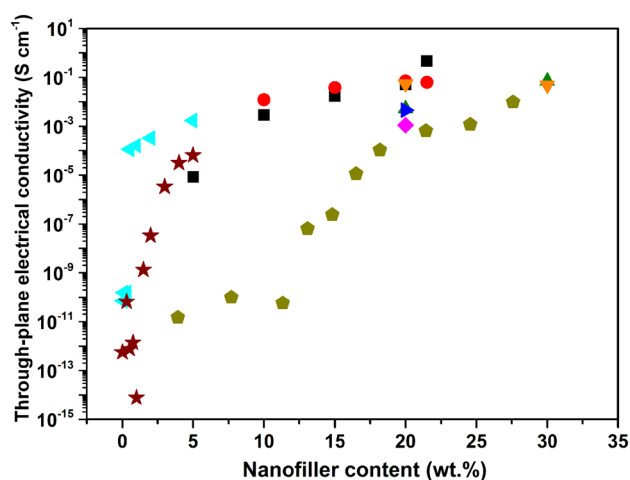


Fig. 4 Measured through-plane electrical conductivity of (■) PP/MWCNT and (●) PP/MWCNT/CNF nanocomposites (present work) and comparison with previous reports by (◀) Tjong et al. (2007), (★) Logakis et al. (2010), and (◆) Shehzad et al. (2013)

exhibit MWCNT agglomerates which cover an increasingly larger fraction of the exposed area with increasing MWCNT content. At higher magnifications, exemplified by the images in Fig. 5g–i, the nanotubes appear well embedded into the matrix, suggesting a good interfacial adhesion to the polymer matrix. For MWCNT contents of 5 and 10 wt%, Fig. 5b, c, g, the MWCNT agglomerates, of a few microns in size, are present in localized areas and it is not possible to ascertain that an effective connectivity exists among them. With higher MWCNT content (15–21.5 wt%), the connectivity among MWCNT throughout the nanocomposite was obviously favored, thus enabling the formation of conductive networks. Basically, the same above observations can be gathered from the SEM images of reprocessed specimens (not shown), although qualitatively a somewhat more homogeneous dispersion of the MWCNT agglomerates was suggested.

The SEM observations are mostly limited to the near surface of the specimens, but the use of CSLM allow some insight of the microstructure at some depth (10–20 μm) inside the composite specimens (Yazdani et al. 2014; Smith et al. 2015; Ilčíková et al. 2016), although at a somewhat lower resolution. Three-dimensional reconstructions of CLSM images of PP/MWCNT nanocomposites, from both original and reprocessed specimens, with different nanofiller contents are shown in Fig. 6a–h. The images were obtained in reflection mode wherein the dark areas correspond mostly to the PP matrix, while the MWCNT can be observed as green, bright features. The images in Fig. 6a, b correspond to PP/5MWCNT and PP/10MWCNT nanocomposites, respectively. At the scale of the CLSM resolution (about 300 nm in all directions), these images indicate a rather uniform distribution of MWCNT agglomerates over most of the analyzed area. Notice that no agglomerates larger than about 10 μm are detected in these samples. On the other hand, when the MWCNT content was increased to 15–21.5 wt%, the distribution of the nanofiller apparently became less uniform and larger agglomerates (10–20 μm) were detected, as illustrated in Fig. 6c–e. Although the electrical conductivity of such samples is indicative of the formation of effective conductive network of MWCNT, their large agglomerates do not constitute an element of an optimized microstructure. On the other hand, after reprocessing, the CLSM images of the PP/15MWCNT-R, PP/20MWCNT-R and PP/21.5MWCNT-R nanocomposites, shown in Fig. 6f–h, give evidence of a reduction in the size of the nanotube agglomerates, in agreement with the significantly higher conductivity values measured in these reprocessed specimens (Table 2).

PP/CNF and PP/MWCNT/CNF nanocomposites

The concept of hybrid systems in nanocomposites, which combine the properties of two or more nanofillers, has been investigated to formulate polymer nanocomposites

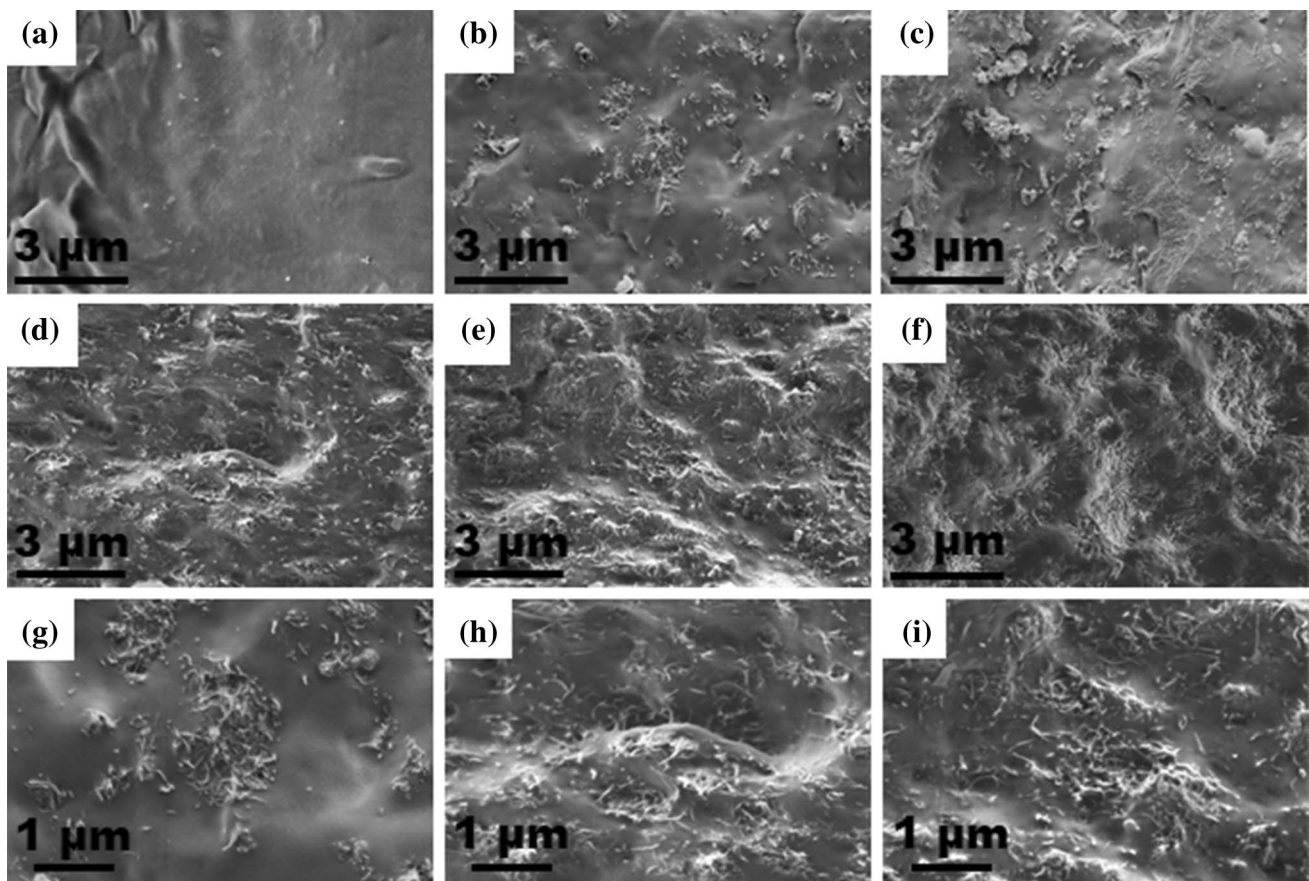


Fig. 5 SEM images of **a** PP without nanofillers, **b** PP/5MWCNT, **c** PP/10MWCNT, **d** PP/15MWCNT, **e** PP/20MWCNT and **f** PP/21.5MWCNT nanocomposites. Images at higher magnifications correspond to **g** PP/5MWCNT, **h** PP/15MWCNT and **i** PP/20MWCNT nanocomposites

with the lowest possible nanofiller content but maintaining a competitive balance of properties (Li et al. 2008; Sun et al. 2009; Garzón and Palza 2014; Liu et al. 2014; Sharma et al. 2016; Lin et al. 2016). In our case, we hypothesized that the electrical conductivity of the PP/MWCNT could be improved if an additional microstructural element of considerable longer dimensions than the nanotubes were homogeneously dispersed in the polymer matrix. Therefore, PP/10MWCNT/10CNF and PP/15MWCNT/15CNF nanocomposites were included in the present study, together with a PP/20CNF nanocomposite used as a reference of the effect of the addition of CNF alone.

The values of in-plane and through-plane electrical conductivities of the CNF-containing nanocomposites are reported in Table 2 and shown in Figs. 2a and 4, respectively, together with the values obtained for PP/MWCNT nanocomposites. The results of in-plane and through-plane conductivity measurements (Table 2, Figs. 2a and 4) on non-reprocessed samples do not reflect any substantial advantage of the CNF addition. However, after reprocessing, in terms of total nanofiller content, the hybrid nanocomposite with 20 wt% content reaches almost the same in-plane

electrical conductivity than the PP/20MWCNT-R nanocomposite, and the latter materials reach substantially higher conductivities than the PP/20CNF nanocomposite. In turn, the PP/15MWCNT/15CNF-R (reprocessed) nanocomposite displayed the highest in-plane electrical conductivity of all specimens produced in the present work: 8.2 S cm^{-1} . It is clear from these results that the addition of CNF together with MWCNT in our samples produced beneficial effects in terms of the in-plane electrical conductivity, particularly in reprocessed nanocomposites. Notice also that the hybrid materials allowed the use of a larger content of total nanofiller content (and, thus, a higher electrical conductivity) than the use of MWCNT alone.

As previously mentioned in the Experimental section, the results of through-plane conductivity measurements on reprocessed samples (which varied in thickness in the range 0.1–0.2 mm) showed a dependence on the thickness of the specimens. Although in general, we could observe an increase in through-plane conductivity with the reprocessing treatment, we abstain from reporting the calculated values for the reprocessed samples until the thickness is fully clarified.

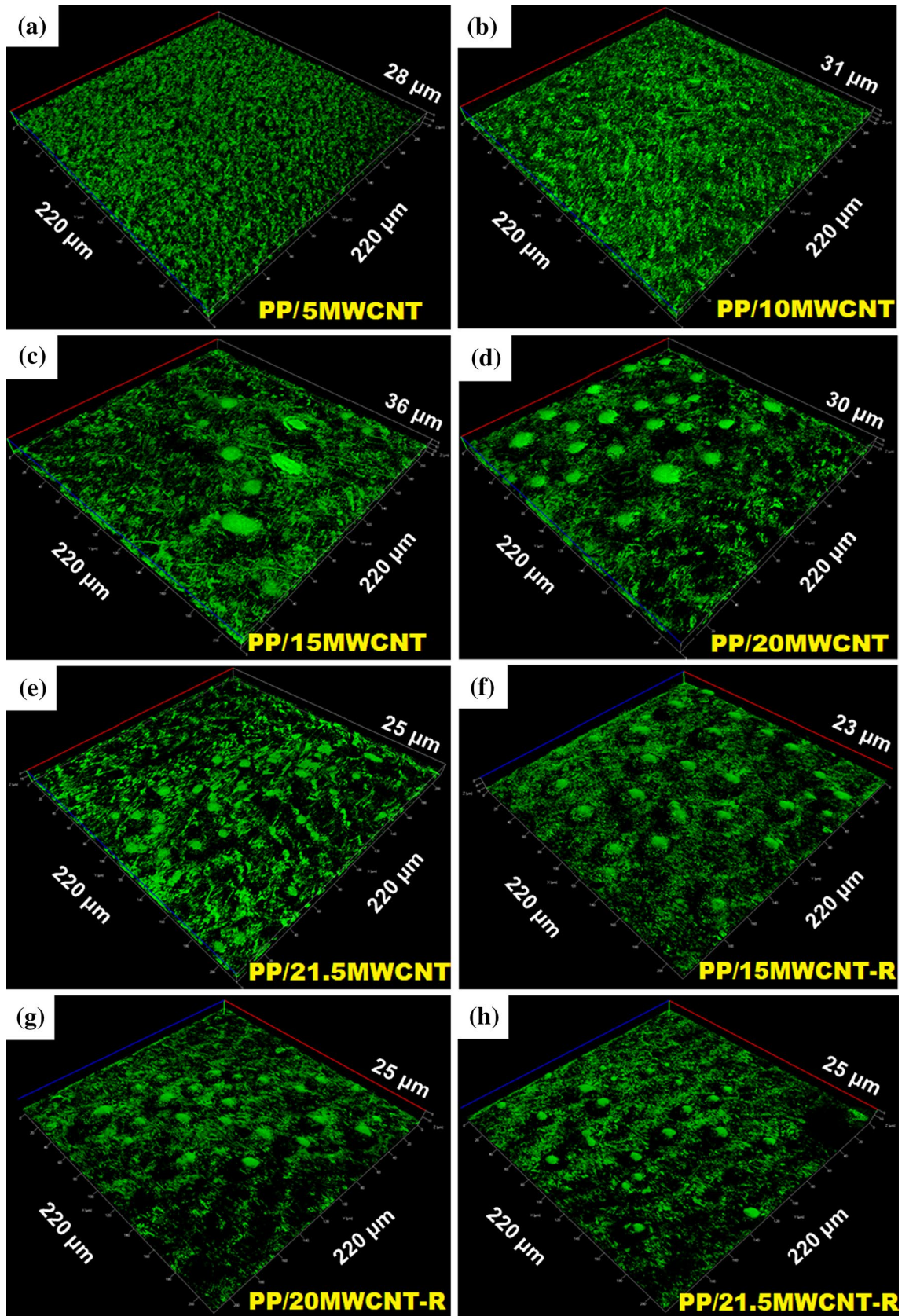


Fig. 6 CLSM images of nanocomposites: **a** PP/5MWCNT, **b** PP/10MWCNT, **c** PP/15MWCNT, **d** PP/20MWCNT, **e** PP/21.5MWCNT, **f** PP/15MWCNT-R, **g** PP/20MWCNT-R, and **h** PP/21.5MWCNT-R

The micrographs of the cryo-fractured surfaces of the CNF-containing nanocomposites, shown in Fig. 7, basically show that (i) the CNF are well-dispersed within the PP matrix and (ii) there is evidence of multiple pull-out occurrences on the fracture area, the latter pointing to a weak link between CNF and the polymer matrix. Even at higher magnifications (not shown), it is difficult to clearly observe the expected connectivity between MWCNT and CNF in these SEM micrographs.

On the other hand, the CLSM image corresponding to the nanocomposite loaded with 20 wt% CNF (Fig. 8a) shows that the filler is evenly distributed over most of the volume of the polymer matrix; since the CNF did not have a clear tendency to agglomerate (see Fig. 7a), this represents a uniform distribution of well-dispersed CNF. In the case of the hybrid nanocomposites combining MWCNT and CNF, the CLSM images shown in Fig. 8b, c also point to a uniform distribution of both nanofillers; moreover, in contrast to the

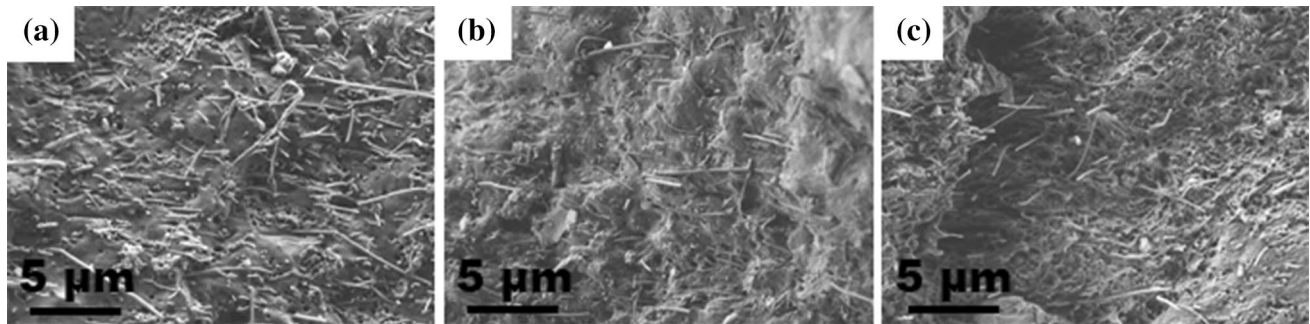


Fig. 7 SEM images of a PP/20CNF, b PP/MWCNT/10CNF and c PP/15MWCNT/15CNF nanocomposites

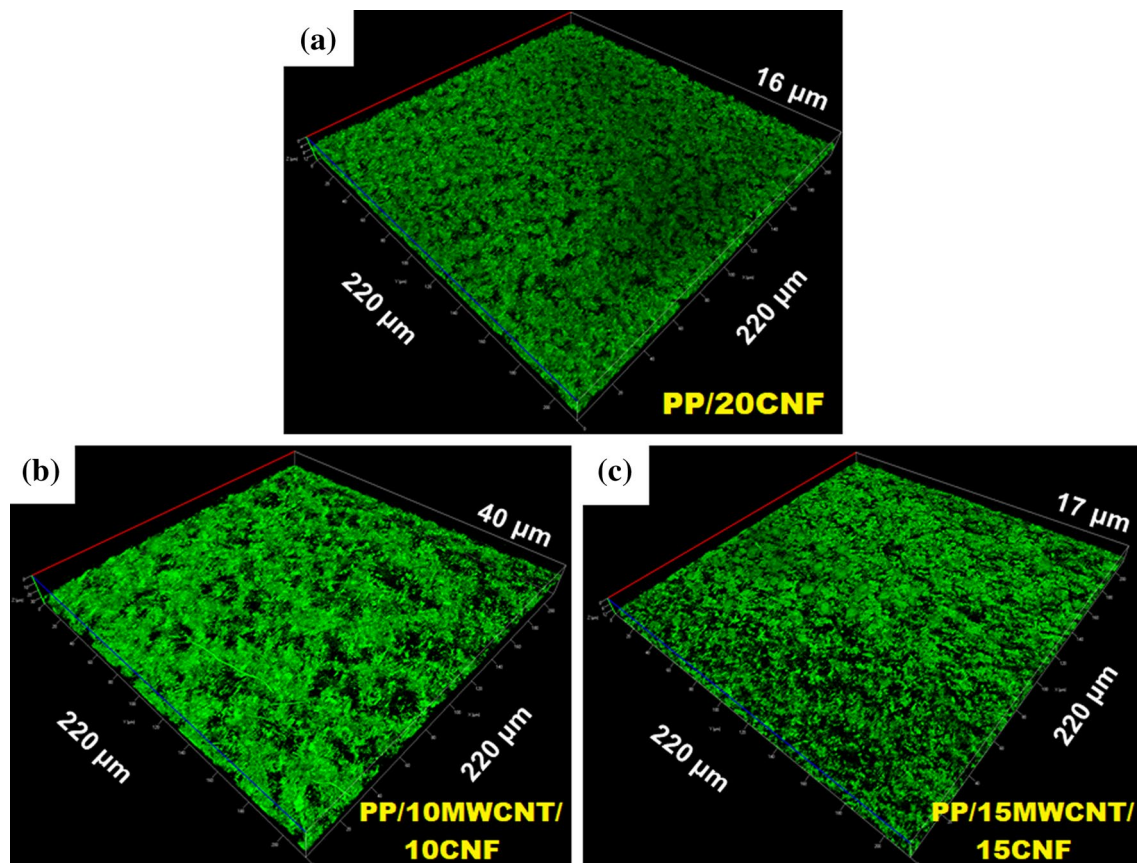


Fig. 8 CLSM images of a PP/20CNF, b PP/10MWCNT/10CNF and c PP/15MWCNT/15CNF nanocomposites

PP/MWCNT composites of high nanofiller content, the size of the MWCNT agglomerates does not seem to exceed a few micrometers.

Microstructure and electrical properties of the nanocomposites

As shown by the results of our electrical measurements, as well as the analysis of similar data from previous works (Zhou et al. 2006; Tjong et al. 2007; Mičušík et al. 2009; Logakis et al. 2010; Pan et al. 2010; Pan and Li 2013; Shehzad et al. 2013; Park et al. 2014; Verma et al. 2015; Al-Saleh 2015, 2016), the highest conductivities achieved in PP/MWCNT nanocomposites are in the range 1.0–10.0 S cm⁻¹. It seems also clear that these maximum values are imposed by the practical restriction in the amount of MWCNT that can be added to the polymer (~20 wt%) in the mixing operation, as the effective volume of the nanofiller addition becomes similar to the volume of the polymer matrix itself. Our results with PP/MWCNT/CNF nanocomposites also indicate that a combined load of MWCNT and CNF nanofillers can produce similar electrical conductivities with the same total nanofiller content (especially in reprocessed nanocomposites). Perhaps more important from a practical perspective is the possibility of increasing the total nanofiller content beyond 20 wt% by partial substitution of MWCNT by CNF. Thus, the PP/15MWCNT/15CNF nanocomposite had a 30 wt% total nanofiller content and actually displayed the highest in-plane electrical conductivity of all our samples (after reprocessing). Compared to the reprocessed PP/21.5MWCNT nanocomposite, it is clear that the increase in conductivity is relatively modest in the reprocessed PP/15MWCNT/15CNF nanocomposite, in spite of a total nanofiller content increase of 8.5 wt%; however, the fact is that the nanofiller content could be increased to 30 wt% by combining the two different nanofillers.

The CLSM and, to a certain point, SEM observations have been useful to confirm the role of the microstructure in the search for high electrical conductivity. A certain degree of MWCNT agglomeration is needed to provide continuous pathways for electron conduction throughout the nanocomposite volume. However, according to the CLSM images in Figs. 6 and 8, an optimized microstructure should avoid MWCNT agglomerates larger than about 10–20 μm. This becomes more difficult as the amount of MWCNT increases (Fig. 6). Notice that the addition of CNF apparently had the effect of preventing the formation of MWCNT agglomerates larger than about 10 μm (Fig. 8), but the analysis of the CLSM images probably requires a more detailed knowledge of the way in which MWCNT and CNF differently contribute to the scattering of the laser radiation when embedded in the polymer matrix.

Inspired by previous reports (Garzón and Palza 2014; Pan et al. 2010), the application of a second processing cycle to the original nanocomposites very clearly eliminated the larger MWCNT agglomerates (Fig. 6) and increased the electrical conductivity of the nanocomposites. As already mentioned, reprocessing led to a reduction in the size of the MWCNT agglomerates (compare Fig. 6c–e to f–h).

Conclusions

PP/MWCNT and PP/MWCNT/CNF nanocomposites have been prepared by melt mixing using different contents of MWCNT and CNF. When used alone, the highest content that could be incorporated in the PP matrix was 21.5 wt%. A clear correlation of the nanocomposite microstructure and the electrical conductivity has been established, particularly for the highest nanofiller contents. In these cases, maximum conductivities require that the MWCNT did not form agglomerates larger than about 10 μm in size. This could be achieved by subjecting the melt mixed and hot pressed materials to a reprocessing operation. Under such circumstances, maximum in-plane and through-plane conductivities of 6.7 and 0.24 S cm⁻¹ were obtained for a MWCNT content of 21.5 wt%. These results are in agreement with the few previous investigations involving PP/MWCNT nanocomposites with nanofiller contents greater than 15 wt%.

The addition of CNF to form hybrid PP/MWCNT/CNF nanocomposites, although not as effective compared to the MWCNT, did allow it to increase to 30 wt% the total amount of nanofiller incorporated in the PP matrix. This, in turn, led to further increase in electrical conductivity, which reached a maximum in the reprocessed PP/15MWCNT/15CNF nanocomposite. This result was consistent with the decrease in the size of MWCNT agglomerates brought about by the CNF addition.

Acknowledgments C. A. Ramírez-Herrera is grateful to Consejo Nacional de Ciencia y Tecnología (CONACYT) for a graduate fellowship with registry number 258940. The authors acknowledge the financial support provided by the 221795-SEP CONACYT project and Centro de Investigación y de Estudios Avanzados del I.P.N. (CINVESTAV-IPN). Centro de Nanociencias y Micro y Nanotecnologías del I.P.N. (CNMN-IPN), LANE-CINVESTAV, Indelpro S.A. de C.V., R. Gómez-Aguilar from ESFM-IPN, B. Zeifert from ESIQIE-IPN, J. L. Reyes-Rodríguez and Z. Rivera-Álvarez from CINVESTAV-IPN are recognized for the technical and experimental support provided in the realization of this research.

Compliance with ethical standards

Conflict of interest On behalf of all authors, the corresponding author states that there is no conflict of interest.

References

- Al-Saleh MH (2015) Electrically conductive carbon nanotube/polypropylene nanocomposite with improved mechanical properties. *Mater Des* 85:76–81. <https://doi.org/10.1016/j.matdes.2015.06.162>
- Al-Saleh MH (2016) Carbon nanotube-filled polypropylene/polyethylene blends: compatibilization and electrical properties. *Polym Bull* 73(4):975–987. <https://doi.org/10.1007/s00289-015-1530-1>
- Al-Saleh MH, Sundararaj U (2009) A review of vapor grown carbon nanofiber/polymer conductive composites. *Carbon* 47(1):2–22. <https://doi.org/10.1016/j.carbon.2008.09.039>
- Bao Y, Xu L, Pang H, Yan D-X, Chen C, Zhang W-Q, Tang J-H, Li Z-M (2013) Preparation and properties of carbon black/polymer composites with segregated and double-percolated network structures. *J Mater Sci* 48(14):4892–4898. <https://doi.org/10.1007/s10853-013-7269-x>
- Bauhofer W, Kovacs JZ (2009) A review and analysis of electrical percolation in carbon nanotube polymer composites. *Compos Sci Technol* 69(10):1486–1498. <https://doi.org/10.1016/j.compscitech.2008.06.018>
- Bikiaris D (2010) Microstructure and properties of polypropylene/carbon nanotube nanocomposites. *Materials* 3(4):2884–2946. <https://doi.org/10.3390/ma3042884>
- Cesano F, Zaccone M, Armentano I, Cravanzola S, Muscuso L, Torre L, Kenny JM, Monti M, Scarano D (2016) Relationship between morphology and electrical properties in PP/MWCNT composites: processing-induced anisotropic percolation threshold. *Mater Chem Phys* 180:284–290. <https://doi.org/10.1016/j.matchemphys.2016.06.009>
- Chodák I, Omastová M, Pionteck J (2001) Relation between electrical and mechanical properties of conducting polymer composites. *J Appl Polym Sci* 82(8):1903–1906. <https://doi.org/10.1002/app.2035>
- Das TK, Prusty S (2013) Graphene-based polymer composites and their applications. *Polym Plast Technol Eng* 52(4):319–331. <https://doi.org/10.1080/03602559.2012.751410>
- Deng H, Zhang R, Bilotti E, Loos J, Peijs T (2009) Conductive polymer tape containing highly oriented carbon nanofillers. *J Appl Polym Sci* 113(2):742–751. <https://doi.org/10.1002/app.29624>
- Garzón C, Palza H (2014) Electrical behavior of polypropylene composites melt mixed with carbon-based particles: effect of the kind of particle and annealing process. *Compos Sci Technol* 99:117–123. <https://doi.org/10.1016/j.compscitech.2014.05.018>
- Ilčíková M, Danko M, Doroshenko M, Best A, Mrlík M, Csomorová K, Šlouf M, Chorvát D Jr, Koynov K, Mosnáčeka J (2016) Visualization of carbon nanotubes dispersion in composite by using confocal laser scanning microscopy. *Eur Polym J* 79:187–197. <https://doi.org/10.1016/j.eurpolymj.2016.02.015>
- Kim H, Abdala AA, Macosko CW (2010) Graphene/polymer nanocomposites. *Macromolecules* 43(16):6515–6530. <https://doi.org/10.1021/ma100572e>
- Kissel WJ, Han JH, Meyer JA (2003) Polypropylene: structure, properties, manufacturing processes and applications. In: Karian HG (ed) *Handbook of polypropylene and polypropylene composites*, 2nd edn. Marcel Dekker Inc., New York, pp 10–27
- Kurahatti RV, Surendranathan AO, Kori SA, Singh N, Kumar AVR, Srivastava S (2010) Defence applications of polymer nanocomposites. *Def Sci J* 60(5):551–563. <https://doi.org/10.14429/dsj.60.578>
- Li J, Wong P-S, Kim J-K (2008) Hybrid nanocomposites containing carbon nanotubes and graphite nanoplatelets. *Mater Sci Eng A* 483–484:660–663. <https://doi.org/10.1016/j.msea.2006.08.145>
- Li Y, Zhu J, Wei S, Ryu J, Wang Q, Sun L, Guo Z (2011) Poly(propylene) nanocomposites containing various carbon nanostructures. *Macromol Chem Phys* 212(22):2429–2438. <https://doi.org/10.1002/macp.201100364>
- Lin J-H, Lin Z-I, Pan Y-J, Chen C-K, Huang C-L, Huang C-H, Lou C-W (2016) Improvement in mechanical properties and electromagnetic interference shielding effectiveness of PVA-based composites: synergistic effect between graphene nano-sheets and multi-walled carbon nanotubes. *Macromol Mater Eng* 301(2):199–211. <https://doi.org/10.1002/mame.201500314>
- Liu T, Wang Y, Eyler A, Zhong W-H (2014) Synergistic effects of hybrid graphitic nanofillers on simultaneously enhanced wear and mechanical properties of polymer nanocomposites. *Eur Polym J* 55:210–221. <https://doi.org/10.1016/j.eurpolymj.2014.04.002>
- Logakis E, Pollatos E, Pandis Ch, Peoglos V, Zuburtikudis I, Delides CG, Vatalis A, Gjoka M, Syskakis E, Viras K, Pissis P (2010) Structure-property relationships in isotactic polypropylene/multi-walled carbon nanotubes nanocomposites. *Compos Sci Technol* 70(2):328–335. <https://doi.org/10.1016/j.compscitech.2009.10.023>
- Merzouki A, Haddaoui N (2012) Electrical conductivity modeling of polypropylene composites filled with carbon black and acetylene black. *ISRN Polymer Sci* 2012:1–7. <https://doi.org/10.5402/2012/493065>
- Mičušik M, Omastová M, Krupa I, Prokeš J, Pissis P, Logakis E, Pandis C, Pötschke P, Pionteck J (2009) A comparative study on the electrical and mechanical behaviour of multi-walled carbon nanotube composites prepared by diluting a masterbatch with various types of polypropylenes. *J Appl Polym Sci* 113(4):2536–2551. <https://doi.org/10.1002/app.30418>
- Müller K, Bugnicourt E, Latorre M, Jorda M, Echegoyen Sanz Y, Lagaron JM, Miesbauer O, Bianchin A, Hankin S, Bözl U, Pérez G, Jesdinszki M, Lindner M, Scheuerer Z, Castelló S, Schmid M (2017) Review on the processing and properties of polymer nanocomposites and nanocoatings and their applications in the packaging, automotive and solar energy fields. *Nanomaterials* 7(4):74. <https://doi.org/10.3390/nano7040074>
- Njuguna J, Pielichowski K, Fan J (2012) Polymer nanocomposites for aerospace applications. In: Gao F (ed) *Advances in polymer nanocomposites: types and applications*. Woodhead Publishing Limited, Cambridge, pp 472–539. 10.1533/9780857096241.3.472
- NOVA 2.1 version 2016.11.15, Metrohm Autolab B. V. (2016) <http://www.ecochemie.nl/news/NOVA21.html>
- Pan Y, Li L (2013) Percolation and gel-like behavior of multiwalled carbon nanotube/polypropylene composites influenced by nanotube aspect ratio. *Polymer* 54(3):1218–1226. <https://doi.org/10.1016/j.polymer.2012.12.058>
- Pan Y, Li L, Chan SH, Zhao J (2010) Correlation between dispersion state and electrical conductivity of MWCNTs/PP composites prepared by melt blending. *Compos A* 41(3):419–426. <https://doi.org/10.1016/j.compositesa.2009.11.009>
- Park SB, Lee MS, Park M (2014) Study on lowering the percolation threshold of carbon nanotube-filled conductive polypropylene composites. *Carbon Lett* 15(2):117–124. <https://doi.org/10.5714/CL.2014.15.2.117>
- Reyes-Acosta MA, Torres-Huerta AM, Domínguez-Crespo MA, Flores-Vela AI, Dorantes-Rosales HJ, Ramírez-Meneses E (2015) Influence of ZrO₂ nanoparticles and thermal treatment on the properties of PMMA/ZrO₂ hybrid coatings. *J Alloys Compd* 643(S1):S150–S158. <https://doi.org/10.1016/j.jallcom.2014.10.040>
- Schroder DK (2006) *Semiconductor material and device characterization*, 3rd edn. Wiley, New York
- Sharma SK, Gupta V, Tandon RP, Sachdev VK (2016) Synergic effect of graphene and MWCNT fillers on electromagnetic shielding properties of graphene-MWCNT/ABS nanocomposites. *RSC Adv* 6(22):18257–18265. <https://doi.org/10.1039/C5RA23418B>

- Shehzad K, Dang Z-M, Ahmad MN, Sagar RUR, Butt S, Farooq MU, Wang T-B (2013) Effects of carbon nanotubes aspect ratio on the qualitative and quantitative aspects of frequency response of electrical conductivity and dielectric permittivity in the carbon nanotube/polymer composites. *Carbon* 54:105–112. <https://doi.org/10.1016/j.carbon.2012.10.068>
- Smith BE, Yazdani H, Hatami K (2015) Three-dimensional imaging and quantitative analysis of dispersion and mechanical failure in filled nanocomposites. *Compos A* 79:23–29. <https://doi.org/10.1016/j.compositesa.2015.08.019>
- Spitalsky Z, Tasis D, Papagelis K, Galiotis C (2010) Carbon nanotube-polymer composites: chemistry, processing, mechanical and electrical properties. *Prog Polym Sci* 35(3):357–401. <https://doi.org/10.1016/j.progpolymsci.2009.09.003>
- Sun Y, Bao H-D, Guo Z-X, Yu J (2009) Modeling of the electrical percolation of mixed carbon fillers in polymer-based composites. *Macromolecules* 42(1):459–463. <https://doi.org/10.1021/ma8023188>
- Tchmutin IA, Ponomarenko AT, Krinichnaya EP, Kozub GI, Efimov ON (2003) Electrical properties of composites based on conjugated polymers and conductive fillers. *Carbon* 41(7):1391–1395. [https://doi.org/10.1016/S0008-6223\(03\)00067-8](https://doi.org/10.1016/S0008-6223(03)00067-8)
- Tibbetts GG, Lake ML, Strong KL, Rice BP (2007) A review of the fabrication and properties of vapor-grown carbon nanofiber/polymer composites. *Compos Sci Technol* 67(7–8):1709–1718. <https://doi.org/10.1016/j.compscitech.2006.06.015>
- Tjong SC, Liang GD, Bao SP (2007) Electrical behavior of polypropylene/multiwalled carbon nanotube nanocomposites with low percolation threshold. *Scr Mater* 57(6):461–464. <https://doi.org/10.1016/j.scriptamat.2007.05.035>
- Verma P, Saini P, Choudhary V (2015) Designing of carbon nanotube/polymer composites using melt recirculation approach: effect of aspect ratio on mechanical, electrical and EMI shielding response. *Mater Des* 88:269–277. <https://doi.org/10.1016/j.matdes.2015.08.156>
- Xin F, Li L (2012) The role of a silane coupling agent in carbon nanotube/polypropylene composites. *J Compos Mater* 46(26):3267–3275. <https://doi.org/10.1177/0021998312437235>
- Yazdani H, Smith BE, Hatami K (2014) Multiscale 3D dispersion characterization of carbon nanotube filled polymer composites using microscopic imaging and data mining. In: Milne WI, Cole M (eds) *Carbon nanotechnology*, 1st edn. One Central Press (OCP), UK, pp 135–158
- Zhou Z, Wang S, Zhang Y, Zhang Y (2006) Effect of different carbon fillers on the properties of PP composites: comparison of carbon black with multiwalled carbon nanotubes. *J Appl Polym Sci* 102(5):4823–4837. <https://doi.org/10.1002/app.24722>

Publisher's Note Springer Nature remains neutral with regard to jurisdictional claims in published maps and institutional affiliations.